

Elastic relaxations associated with the $Pm\bar{3}m - R\bar{3}c$ transition in LaAlO_3 : IV. An incipient instability below room temperature

This article has been downloaded from IOPscience. Please scroll down to see the full text article.

2010 J. Phys.: Condens. Matter 22 035406

(<http://iopscience.iop.org/0953-8984/22/3/035406>)

[The Table of Contents](#) and [more related content](#) is available

Download details:

IP Address: 38.107.191.97

The article was downloaded on 17/03/2010 at 19:44

Please note that [terms and conditions apply](#).

Elastic relaxations associated with the $Pm\bar{3}m-R\bar{3}c$ transition in LaAlO_3 : IV. An incipient instability below room temperature

M A Carpenter¹, A Buckley¹, P A Taylor¹, R E A McKnight¹ and T W Darling^{2,3}

¹ Department of Earth Sciences, University of Cambridge, Downing Street, Cambridge CB2 3EQ, UK

² Material Science and Technology, Los Alamos National Laboratory, Los Alamos, NM 87545, USA

³ Department of Physics, University of Nevada, Reno, NV 89577, USA

Received 2 August 2009, in final form 13 November 2009

Published 21 December 2009

Online at stacks.iop.org/JPhysCM/22/035406

Abstract

Resonant ultrasound spectroscopy has been used to characterize elastic softening and acoustic dissipation behaviour in single crystal and ceramic samples of LaAlO_3 between 10 and 300 K. For the twinned $R\bar{3}c$ single crystals, average values of the cubic elastic moduli $\frac{1}{2}(C_{11} - C_{12})$ and C_{44} were followed while the ceramic sample provided data for the bulk and shear moduli. A Debye-like dissipation peak occurs in the vicinity of 250 K, from which an activation energy of $43 \pm 6 \text{ kJ mol}^{-1}$ has been obtained. The mechanism for this is not known, but it is associated with C_{44} and therefore could be related in some way to the cubic \leftrightarrow rhombohedral transition at $\sim 817 \text{ K}$. Slight softening in the temperature interval $\sim 220 \rightarrow 70 \text{ K}$ of resonance peaks determined by shear elastic moduli hints at an incipient E_g ferroelastic instability in LaAlO_3 . The softening interval ends with a further dissipation peak at $\sim 60 \text{ K}$, the origin of which is discussed in terms of freezing of atomic motions of La and/or Al away from their high symmetry positions in the $R\bar{3}c$ structure. LaAlO_3 thus shows evidence of incipient structural instability at low temperatures which is potentially analogous with the phenomenologically rich behaviour of SrTiO_3 .

1. Introduction

SrTiO_3 shows a variety of subtle variations in physical properties at temperatures which are well below the $Pm\bar{3}m \leftrightarrow I4/mcm$ octahedral tilting transition at $\sim 106 \text{ K}$ (Müller *et al* 1991, Hehlen *et al* 1996, Scott and Ledbetter 1997, Grupp and Goldman 1997, Arzel *et al* 2002, 2003). These have attracted close interest in relation to the behaviour of the pure phase, itself, but they seem also to be indicative of incipient structural instability which becomes explicit when the composition is changed. Replacing ^{16}O by ^{18}O gives rise to a ferroelectric phase transition (Itoh *et al* 1999, 2004, Itoh and Wang 2000, 2003), and ferroelectric properties are also induced when Sr^{2+} is replaced by Ca^{2+} (Bednorz and Müller 1984), Ba^{2+} (Lemanov *et al* 1996, Ménoret *et al* 2002)

or Cd^{2+} (Guzhva *et al* 1998, 2001) at low concentrations. Chemical doping is, more generally, used to induce or engineer properties for potential applications in device materials. In most of these materials, the key effects are almost certainly associated with the elastic strain relaxations which accompany chemical substitutions and, because of the high sensitivity of single crystal elastic moduli to such relaxations, elasticity represents the property most like to reveal the nature of both explicit and incipient instabilities. For example, the most overt evidence for the unusual structural evolution of SrTiO_3 at low temperatures is provided by anomalies in C_{11} and C_{44} (Hehlen *et al* 1996, Scott and Ledbetter 1997) and the ferroelectric phase transition in $\text{SrTi}^{16}\text{O}_3\text{-SrTi}^{18}\text{O}_3$ is marked by substantial elastic softening of C_{44} (Yamaguchi *et al* 2001, Yagi *et al* 2002). As part of a much larger study of the

elastic and anelastic properties of LaAlO_3 , reported in the three previous papers in this series (Carpenter *et al* 2010c, 2010b, 2010a), Resonant Ultrasound spectra were collected below room temperature. These have provided evidence for an incipient instability which is perhaps analogous to the behaviour of SrTiO_3 and which forms the primary focus of this paper.

Figure 1 is the low temperature part of the phase diagram for the LaAlO_3 – PrAlO_3 solid solution based on experimental data from the literature (Glynn *et al* 1975, Carpenter *et al* 2005, 2009, Basyuk *et al* 2009). It reveals the close proximity of a phase transition to pure LaAlO_3 . In PrAlO_3 , a Jahn–Teller distortion of the Pr^{3+} coordination shell is believed to be responsible for stabilizing both the $Imma$ and $C2/m$ structures. Transition temperatures for both the $R\bar{3}c \leftrightarrow Imma$ and $Imma \leftrightarrow C2/m$ transitions decrease with increasing La content. The $Imma \leftrightarrow C2/m$ transition is pseudoproper ferroelastic in character and the actual transition temperature therefore depends on coupling of the order parameter with the symmetry-breaking strain, which may also decline with increasing La content. The stability field of the $Imma$ structure appears to pinch out, according to the results of Glynn *et al* (1975) and Basyuk *et al* (2009), but it is clear that there could be an intrinsic ferroelastic instability in the close vicinity of LaAlO_3 at low temperatures. Further evidence for at least a non-uniform evolution of the structure at low temperatures is provided by the spontaneous strain due to the $Pm\bar{3}m \leftrightarrow R\bar{3}c$ transition. In the saturation regime, as $T \rightarrow 0$ K, the strain can be described by the expected coth function, but it appears that more than one saturation temperature and, hence, saturation process, is involved (Hayward *et al* 2002). Thus both SrTiO_3 and LaAlO_3 appear to have incipient structural instabilities at low temperatures which influence their structural evolution directly. However, in contrast with the related ferroelectric transition to an orthorhombic phase in SrTiO_3 , the related transition in LaAlO_3 is ferroelastic.

2. Experimental methods

Preparation of the rectangular parallelepipeds of single crystal (4/2002: $3.906 \times 4.440 \times 4.808$ mm³, 0.5263 g) and polycrystalline LaAlO_3 (cer1: $2.660 \times 3.148 \times 3.624$ mm³, 0.1648 g; cer2: $2.662 \times 3.150 \times 3.668$ mm³, 0.1665 g) for the present study has been described in Carpenter *et al* (2010a). The single crystal was originally cut from a larger crystal obtained from the same supplier, Crystal GmbH (Berlin), as had provided material for other studies in the literature and is therefore assumed to have the same chemical and physical characteristics. The ceramic sample, with a density corresponding to $\sim 83\%$ of the single crystal density, was prepared from powder obtained by crushing offcuts of the same larger single crystal sample. Two separate parallelepipeds of the ceramic sample were used because a small fragment must have fallen off cer1 at some point during the heating cycle described by Carpenter *et al* (2010a), before the cooling cycle described here. It was observed to have a small cavity in one face and slightly reduced mass (0.1641 instead of 0.1648 g).

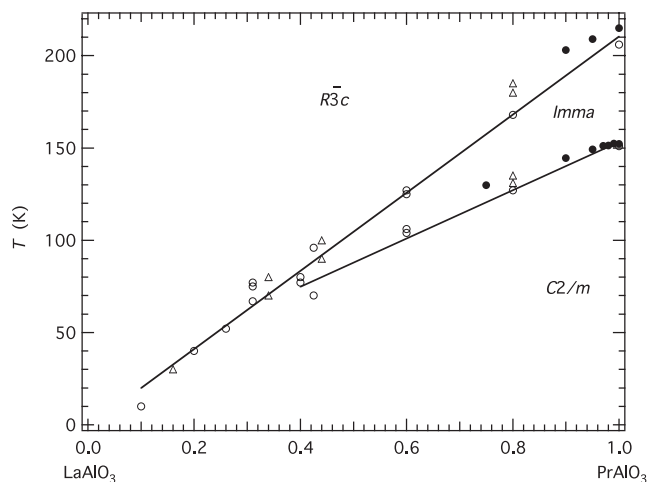


Figure 1. Low temperature part of the subsolidus phase diagram for the $\text{Pr}_{1-x}\text{La}_x\text{AlO}_3$ solid solution. Open circles represent transition temperatures delineating stability fields of $Imma$ and $C2/m$ structures taken from Glynn *et al* (1975). Filled circles are transition temperatures from Carpenter *et al* (2005, 2009). Open triangles are data from Basyuk *et al* (2009). Glynn *et al* (1975) described the lowest temperature structure as being triclinic, but more recent studies have shown that it is monoclinic.

The low temperature RUS instrument in Cambridge has been described in detail by McKnight *et al* (2007). In it, the sample rests across a pair of corners, a pair of edges or a pair of faces between PZT transducers and the head is lowered into an ‘Orange’ helium flow cryostat. Before starting each experiment, the sample chamber was evacuated and then filled with ~ 1 – 3 mbars of helium gas to allow heat exchange with the sample. Temperature was recorded with a silicon diode inside the sample chamber, through a Lakeshore 340 controller. The measured transition temperature of SrTiO_3 in a separate experiment was 106 K, which is indistinguishable from values obtained elsewhere in the literature (e.g. Hayward and Salje 1999). The spectra themselves were collected using dynamic resonance system (DRS) modulus II electronics, during cooling and heating sequences controlled by software produced in-house. Data from the single crystal sample were collected over the frequency range 0.3–1.2 MHz, with 50 000 data points per spectrum. These provided a resolution in frequency of 0.018 kHz. Data from the ceramic samples were collected over the frequency range 0.3–1.8 MHz, with 100 000 data points in the case of cer1 (resolution 0.015 kHz) and 65 000 data points for cer2 (resolution 0.023 kHz).

All spectra were analysed offline within the software package ‘Igor Pro’ (Wavemetrics). As described in detail by Carpenter *et al* (2010a) resonance peak frequencies from the single crystal were measured by inspection and used to calculate elastic moduli, $\frac{1}{2}(C_{11} - C_{12})$, C_{44} , and bulk modulus, $K (= \frac{1}{3}(C_{11} + 2C_{12}))$ using the DRS software described by Migliori *et al* (1993) and Migliori and Sarrao (1997). Quotation marks are used here and below to emphasize that they are cubic averages for a twinned rhombohedral crystal. Lattice parameter data of Hayward *et al* (2005) were used to correct the dimensions of the parallelepipeds for the

influence of thermal expansion. This procedure resulted in fits with rms errors of 0.4–0.7%. The χ^2 matrix for individual elastic moduli showed that the (average) cubic shear elastic moduli, $\frac{1}{2}(C_{11} - C_{12})$ and C_{44} , were tightly constrained by the data. Values of K and the shear modulus, G , for the ceramic sample cer1 were determined in the same way, with rms errors of ~ 0.6 – 0.8% , from fitting to between 31 and 46 peaks. Data for G were more tightly constrained than for K . The slightly less than ‘good’ fits are assumed to be due to anisotropy of grain orientations or to an anisotropic distribution of pore sizes/orientations.

Values of the mechanical quality factor, Q , were determined as $Q = f/\Delta f$, where f is the peak frequency and Δf is the peak width at half maximum height, using an asymmetric Lorentzian function (following the approach of Schreuer *et al* 2003 and Schreuer and Thybaut 2005) to fit selected, individual peaks in the primary spectra.

3. Results

Stacks of spectra for the single crystal (4/2002) and ceramic sample cer1 were shown in figures 1 and 7 of Carpenter *et al* (2010a), respectively, for direct comparison with spectra collected at high temperatures. They had been collected in a heating sequence of 10 K steps from 10 to 280 K (single crystal) and from 10 to 290 K (ceramic), with 10 or 15 min equilibration at each temperature before data collection. Variations in the elastic moduli obtained for 4/2002 and cer1 were included in figures 4 and 8 of Carpenter *et al* (2010a), also for comparison with results from high temperatures. Values of the moduli for 4/2002 are listed here in table 1. Rather than considering fit values of the moduli, however, details of the low temperature region are considered in terms of the raw data. Based on output from the fitting program, resonance peaks selected for analysis depended on $\sim 97\%$ of

Table 1. Single crystal elastic modulus data at different temperatures for LaAlO₃. Inverted commas indicate average cubic values for the rhombohedral phase.

Sample	T (K)	C_{44} (GPa)	$\frac{1}{2}(C_{11} - C_{12})$ (GPa)
4/2002	10.9	143.8	57.7
	20.7	143.7	57.7
	40.5	143.6	57.6
	60.6	143.6	57.7
	80.2	144.1	57.9
	99.7	144.8	58.2
	119.6	145.2	58.6
	139.3	145.5	59.0
	159.0	145.6	59.4
	178.8	146.1	59.7
	198.5	145.6	60.3
	218.2	145.9	60.7
	237.9	146.3	61.0
	257.6	146.2	61.3
	278.1	146.1	61.5
	297.8	145.9	61.6

C_{44} (peak at ~ 0.44 MHz in room temperature spectrum) and $\sim 91\%$ (~ 0.48 MHz peak) or $\sim 100\%$ (~ 0.475 MHz peak) of $\frac{1}{2}(C_{11} - C_{12})$. Variations in the frequencies of these peaks are shown in figure 2. Additional high temperature data from Carpenter *et al* (2010a) have been added in order to reveal the overall trends. For a polycrystalline sample, most of the mechanical resonances are dominated by G , and the frequency variation of a peak near 0.475 MHz at room temperature is illustrated in figure 3. The elastic moduli which determine a given distortional mode scale as f^2 , so that increases and decreases in the frequencies of these peaks indicate softening and stiffening. Values of Q^{-1} from $\Delta f/f$, for the same peaks then indicate the extent of dissipation associated with each of the moduli.

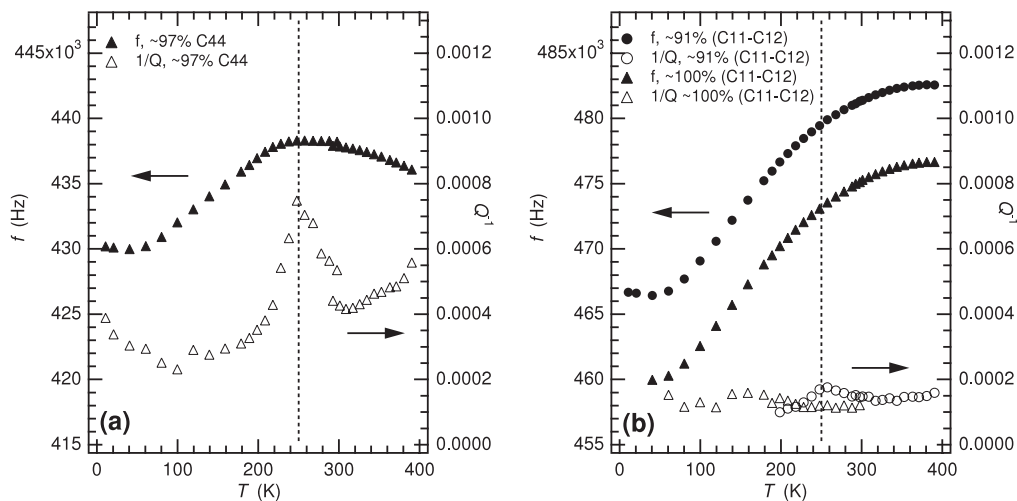


Figure 2. Frequency, f , and inverse mechanical quality factor, Q^{-1} , variations of individual resonance peaks in the temperature interval 10–400 K (crystal 4/2002). (a) A peak dependent on $\sim 97\%$ of C_{44} shows slight softening with falling temperature between 250 and 60 K and a maximum in Q^{-1} at ~ 250 K. (b) Peaks dependent on $\sim 91\%$ and $\sim 100\%$ of $\frac{1}{2}(C_{11} - C_{12})$ also show softening with falling temperature, though this starts from about 400 K. For the 100% $\frac{1}{2}(C_{11} - C_{12})$ peak there is no anomaly in Q^{-1} . For the 91% $\frac{1}{2}(C_{11} - C_{12})$ peak the anomaly at ~ 250 K can be attributed to the slight dependence on C_{44} . Data for Q^{-1} at the lowest temperature become relatively uncertain because the resonance peaks were narrow and weak.

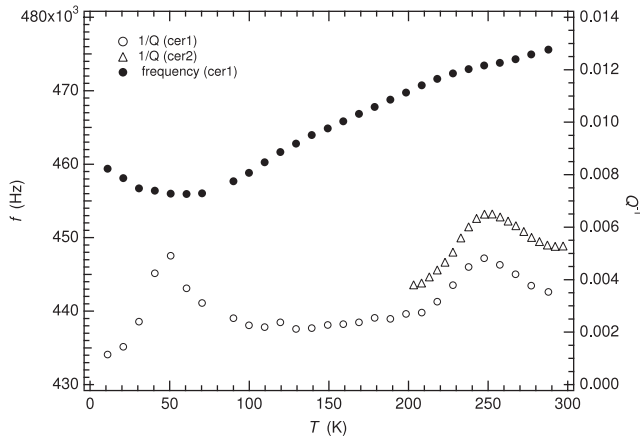


Figure 3. Variation of frequency, f , and Q^{-1} determined for the resonance peak near 0.475 MHz from sample cer1 below room temperature, showing softening down to ~ 70 K and two distinct maxima in Q^{-1} . The low temperature maximum in Q^{-1} correlates with the change from elastic softening to stiffening with falling temperature. The 250 K anomaly in Q^{-1} is possibly accompanied by a slight increase in f (and, hence, in the shear modulus) with falling temperature. Data for Q^{-1} from one of the resonance peaks from cer2 are also shown.

For resonances determined by ‘ C_{44} ’ of the single crystal there is a distinct maximum in Q^{-1} extending between 200 and 300 K and centred on ~ 250 K (figure 2(a)). Below ~ 225 K, the frequency started to reduce. Q^{-1} for the peak calculated to depend 100% on ‘ $\frac{1}{2}(C_{11} - C_{12})$ ’ is completely flat, while the second, depending 91% on ‘ $\frac{1}{2}(C_{11} - C_{12})$ ’ showed a very small anomaly (figure 2(b)), indicating that the dissipation behaviour near 250 K is due exclusively to resonance phenomena associated with ‘ C_{44} ’. For peaks determined by ‘ $\frac{1}{2}(C_{11} - C_{12})$ ’ a trend of reducing frequency with falling temperature established at higher temperatures continued through this interval (figure 2(b)). As is also evident from the stack of spectra shown in figure 1 of Carpenter *et al* (2010a), the reduction in peak frequencies with falling temperature levels off at ~ 60 – 70 K. Q^{-1} perhaps also increases slightly. An attempt was made to measure the temperature dependence of Q^{-1} peak for ‘ C_{44} ’ from resonances with different frequencies in order to determine the temperature/frequency properties of the dissipation process at 200–300 K. This yielded indeterminate results, however, because the peaks are exceptionally sharp and include slight tails which indicate that ringing from one measuring frequency had not completely decayed before measurement of the next.

As expected, the ~ 0.475 MHz resonance peak of cer1 shows the same variation of frequency with temperature as would be shown by a combination of ‘ $\frac{1}{2}(C_{11} - C_{12})$ ’ and ‘ C_{44} ’ (figure 3). Q^{-1} has two distinct maxima, centred on ~ 60 and ~ 250 K. The 250 K anomaly is accompanied by a small increase in peak frequency with falling temperature, but then decreases before levelling off at ~ 70 – 80 K and increasing slightly below ~ 50 K. As shown in figure 8 of Carpenter *et al* (2010a), K also shows a slight softening with falling temperature, though the total change is probably less than the experimental uncertainty of the absolute values.

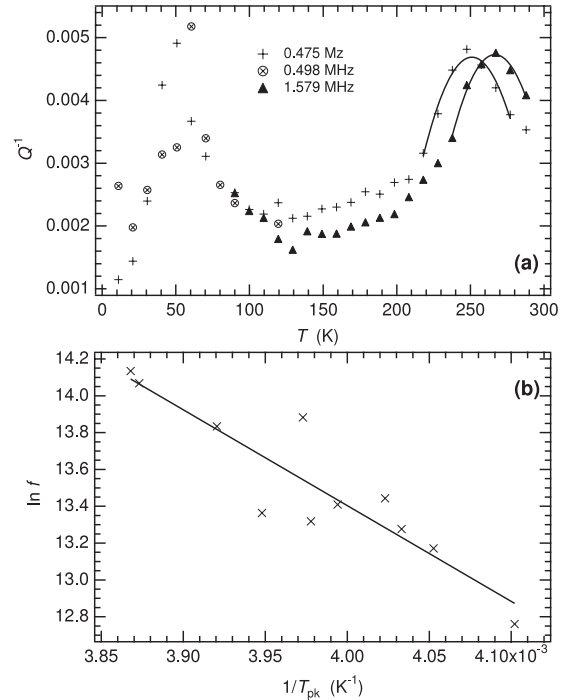


Figure 4. Characteristics of the peak in Q^{-1} near 250 K determined from different resonance peaks in spectra from ceramic samples. (a) Data from cer1. The temperature at which Q^{-1} reaches a maximum, T_{pk} , near 250 K is clearly frequency dependent (curves are guides to the eye). There is a second peak in Q^{-1} at ~ 60 K. (b) Data from cer2. Arrhenius plot of T_{pk} from maxima in Q^{-1} of the type shown in (a) and frequency, f , of the resonance peaks from which the Q^{-1} data were obtained. The slope of the straight line gives an activation energy of 43 ± 6 kJ mol $^{-1}$.

Because of the higher absolute values of Q^{-1} for the ceramic samples, it has been possible to get good full width at half maximum height data for resonance peaks in the low temperature spectra. Variations in Q^{-1} as a function of temperature through the 250 K anomaly for selected resonance peaks from the first ceramic sample were found to be frequency dependent (figure 4(a)). This dependence was then investigated in detail using data collected at 5 K intervals between ~ 200 and ~ 310 K from the second ceramic sample (cer2). For each of the resonance peaks, the variation of Q^{-1} was followed as a function of temperature in order to find the temperature, T_{pk} , at which it reached a maximum value. Interpolation between data points was achieved simply by using the same asymmetric Lorentzian function as been used to fit the individual resonance peaks. The results of this analysis are plotted in Arrhenius form ($\ln(\text{resonance frequency, } f)$ versus $1/T_{pk}$) in figure 4(b) where they define a straight line. Assuming thermal activation described by

$$f = f_0 \exp\left(\frac{-E}{RT_{pk}}\right), \quad (1)$$

the linear fit shown gives $E = 43 \pm 6$ kJ mol $^{-1}$, $\ln f_0 = 37 \pm 3$ ($f_0 \sim 7 \times 10^{14}$ Hz). Resonance peaks in the temperature interval of the 50 K anomaly were too noisy to allow an equivalent analysis, but the maximum in Q^{-1} was at least qualitatively reproducible for different resonance

peaks (figure 4(a)). The 250 K anomaly is accompanied by an increase in frequency of the 0.475 MHz peak which corresponds to an increase of ~ 0.4 GPa in G with falling temperature. The 50 K anomaly is clearly associated with an upturn of the temperature dependence of the shear modulus.

4. Discussion

4.1. 250 K anomaly

The RUS results for low temperatures presented here complement measurements of other properties (Hayward *et al* 2002, 2005) in showing that the structural evolution of LaAlO₃ below room temperature is not the smooth variation associated with normal thermal expansion and saturation as $T \rightarrow 0$ K. In particular, the Debye-like peak in Q^{-1} for ‘ C_{44} ’ resonance peaks at ~ 250 K coincides with breaks in slope of structural parameters from refinements of neutron diffraction data. For example, figures 10 and 12 of Hayward *et al* (2005) both show small breaks in slope near ~ 250 K indicating changes in the temperature evolution of the octahedral tilt angle, the octahedral distortion parameter and the symmetry-breaking strain relative to each other. At about the same temperature, the variation of the squared frequency of the E_g soft mode shows a marked change from the trend established for e_4 (figure 3(b) of Carpenter *et al* 2010b); the non-symmetry-breaking strain e_1 possibly also shows a small change in trend (figure 1(b) of Carpenter *et al* 2010b). There does not appear to be an anomaly in the heat capacity (Schnelle *et al* 2001), however, which implies the involvement of some relaxation process rather than a discrete phase transition. Luo and Wang (2008) have also used first principles calculations to show that the $R\bar{3}c$ structure should be more stable than $R\bar{3}m$ or $R3c$ at low temperatures. The dependence of the 250 K dissipation only on ‘ C_{44} ’ resonances implies a strain relaxation mechanism which is related to e_4 and, therefore, could be related in some way to the cubic \leftrightarrow rhombohedral phase transition.

Equation (3) of Carpenter *et al* (2010a) can be written as

$$Q^{-1} = Q_{\max}^{-1} \frac{\omega\tau}{1 + \omega^2\tau^2}, \quad (2)$$

where $Q_{\max}^{-1} \approx (C_U - C_R)/2C_R$ and is the value of Q^{-1} when $\omega\tau = 1$ (C_U is the relevant elastic modulus of the unrelaxed state and C_R the modulus for the relaxed state). Since Q_{\max}^{-1} is less than 0.001 for ‘ C_{44} ’ (figure 2(a)) it follows that the relaxation process is expected to cause an increase of $2 \times 0.001 \times 150 = 0.3$ GPa ($=C_U - C_R$) below ~ 250 K in C_{44} , and peak frequency data for the ceramic sample could be understood on this basis (figure 3). There is a total softening of ~ 2.7 GPa in ‘ C_{44} ’ between ~ 220 and ~ 50 K, however (figure 2(a) of this paper and figure 7(a) of Carpenter *et al* 2010a). This is accompanied by softening of ‘ $\frac{1}{2}(C_{11} - C_{12})$ ’ over a wider temperature interval, as if there is softening of E_g acoustic modes of the $R\bar{3}c$ structure. The purely elastic stability limits for a crystal structure with respect to spontaneous distortion are given by the eigenvalues of the elastic modulus matrix (Born and Huang 1954). In the case of crystal class $\bar{3}m$, the condition for stability is

$$(C_{11T} - C_{12T}) C_{44T} - 2C_{14T}^2 > 0, \quad (3)$$

and the velocity, V , of the corresponding soft acoustic modes (with symmetry E_g) would be given by

$$\rho V^2 = \frac{1}{4} \{ (C_{11T} - C_{12T} + 2C_{44T}) - [(C_{11T} - C_{12T} - 2C_{44T})^2 + 16C_{14T}^2]^{1/2} \}. \quad (4)$$

The subscript T indicates moduli defined with respect to the trigonal reference system and ρ is density (Cowley 1976, Carpenter and Salje 1998, Terhune *et al* 1985). With respect to cubic reference axes and considering only average cubic moduli, equation (3) gives $(C_{11} - C_{12})C_{44} \rightarrow 0$ as $T \rightarrow T_c$ for a proper or pseudoproper ferroelastic transition. The observed softening of ‘ $\frac{1}{2}(C_{11} - C_{12})$ ’ and ‘ C_{44} ’ would lead ultimately to a monoclinic ($C2/c$) or triclinic ($P\bar{1}$) structure, but the softening trend is reversed at ~ 60 K. A further dissipation peak at this temperature suggests that the change in lattice dynamics is associated with a final relaxation process.

Glynn *et al* (1975) reported that the low temperature phase in (La, Pr)AlO₃ has triclinic symmetry. Subsequent studies of the Pr-rich end of the solid solution have shown that this is in fact monoclinic, with space group $C2/m$ (Moussa *et al* 2001, Carpenter *et al* 2005, Basyuk *et al* 2009). Basyuk *et al* (2009) have shown that the stability field of the monoclinic structure could extend to within a few % of LaAlO₃. The $C2/m$ phase of PrAlO₃ is believed to be stabilized by a cooperative Jahn–Teller distortion (Birgeneau *et al* 1974) which should not exist in LaAlO₃ owing to its different electronic structure. The evidence of elastic softening, although not great in extent, suggests that there is an incipient ferroelastic instability even in LaAlO₃, however.

The activation energy of ~ 43 kJ mol⁻¹ obtained from the 250 K Debye-like peak is too large to be due entirely to a barrier between closely spaced cation positions within individual coordination polyhedra, but too small to be due to migration of oxygen vacancies. The behaviour more nearly resembles that of protons in metals. Leisure *et al* (2004) obtained ~ 22 kJ mol⁻¹ for H motion in TaV₂H_{0.53} from resonance peaks near ~ 1 MHz and ~ 250 K, for example. The impurity content of the LaAlO₃ crystals used in the present study has not been determined but, on the other hand, the 250 K dissipation peak in LaAlO₃ also coincides with the onset of the softening interval, ~ 250 – 60 K, for ‘ C_{44} ’ (figure 2(a)) and the other anomalies such as the saturation behaviour of the E_g soft optic mode (Hayward *et al* 2002). It is difficult to reconcile this correlation simply as being due to changes in the dynamics of impurity elements or other low concentration defects.

4.2. 70 K anomaly

Some additional evidence for the nature of the structural behaviour near 70 K is provided by the work of Zuccaro *et al* (1997) and McN Alford *et al* (2001), who observed Debye-like relaxation peaks below room temperature in single crystal and ceramic samples of LaAlO₃ using dielectric resonance techniques at ~ 1 – 10 GHz. The description of a peak at ~ 70 K, assuming thermal activation according to equations (1) with $E \approx 3$ kJ mol⁻¹ and $f_0 \approx 3 \times 10^{12}$, led Zuccaro *et al* (1997) to conclude that the dissipation is due to motion of atoms between different local energy minima within individual

sites. The dissipation process could be due to freezing of atomic motions of La or Al amongst different positions within individual coordination polyhedra away from their high symmetry positions. The energy barrier between such positions would be on the order of the enthalpy difference between twin domains as given by the Landau expansion for the transition. At low temperatures this would be ~ 0.5 – 1 kJ mol⁻¹, according to the calibration of Carpenter *et al* (2010b).

Two further pieces of evidence provide clues that the relaxation and acoustic softening processes could be related to changes from dynamic to static disorder for displacements of Al and/or La from their high symmetry positions in the $R\bar{3}c$ structure. Firstly, the excess entropy for the cubic \leftrightarrow rhombohedral transition is larger than normal for a pure tilting transition. For example, the a coefficient for the cubic \leftrightarrow tetragonal transition in SrTiO₃ is 0.65 J mol⁻¹ (Hayward and Salje 1999, Carpenter 2007), giving a total excess entropy at order parameter $Q = 1$ of ~ 0.33 J mol⁻¹ K⁻¹. For LaAlO₃ $a = 3.9$ J mol⁻¹ K⁻¹ and the equivalent total excess entropy would be ~ 1.95 J mol⁻¹ K⁻¹, suggesting some contribution from configurational effects. Secondly, Sathe and Dubey (2007) observed a weak additional peak in Raman spectra which displayed increasing intensity below ~ 240 K. They associated this with other weak peaks at higher temperatures and considered the possibility that the local symmetry could be $R3c$ or $R\bar{3}$, due to displacements of La and Al from their high symmetry positions in the $R\bar{3}c$ structure.

According to Howard *et al* (2000) AlO₆ octahedra in LaAlO₃ suffer a slight compression between triangular faces aligned perpendicular to [111] of the cubic parent structure and a slight expansion in the plane perpendicular to this. Displacements of Al from the centre of the octahedra parallel to [111] are therefore unlikely, but could still occur in the directions of the apices of the octahedra. In a disordered distribution of such displacements, there would be three equivalent sites just above the centre of the octahedron and three just below, rotated through 60° so as to be consistent with the $\bar{3}$ axis. If the exchange between sites occurs on a timescale slower than optical phonon frequencies, the Raman spectra would reveal a tendency for the local symmetry to be less than $R\bar{3}c$. The exchange frequencies (also for La distributed between sites away from the high symmetry position) should reduce with falling temperature and must freeze out at some point, depending on the height of energy barriers between the sites. The slowing down of these motions could contribute to the E_g acoustic mode softening and a change from dynamic to static disorder (or some degree of local static order) below ~ 60 K would result in a reversion to normal stiffening with falling temperature. Variations in the order parameter saturation temperature reported by Hayward *et al* (2002) are thus due to a complex series of relaxation processes.

5. Conclusions

Although a definitive explanation of the elastic and anelastic anomalies has not been offered, the existence of an incipient

ferroelastic instability in LaAlO₃ would have implications for how it might behave under stress. Imposing a rhombohedral strain on tetragonal SrTiO₃ results in a monoclinic structure with $C2/c$ symmetry (Müller *et al* 1970, Carpenter 2007). Similarly, the encroachment of tetragonal and rhombohedral stability fields in PZT results in the stabilization of a monoclinic structure at the morphotropic phase boundary (Noheda 2002). In this case, enhanced ferroelectric and piezoelectric properties result. Structural relaxations under the influence of stress must also be important in the topical sandwich materials made of alternating layers of LaAlO₃ and SrTiO₃ (e.g. Schwingenschlögl and Schuster 2009, Huijben *et al* 2009). In a sandwich of SrTiO₃, with its susceptibility towards tetragonal distortion, and LaAlO₃ with rhombohedral lattice geometry, the combined stress fields arising from lattice mismatches could favour monoclinic distortions in both phases. Such structural relaxations might then be a contributory factor in the remarkable properties shown by the interfaces between these materials. If the SrTiO₃ is doped or has ¹⁸O replacing ¹⁶O and the LaAlO₃ is also doped, the sandwich would constitute a material with incipient ferroelectric, relaxor and ferroelastic instabilities which could all be controlled by the choice of composition, temperature, stress and electric field.

Acknowledgments

Elasticity measurements on LaAlO₃ have been supported by The Natural Environment Research Council of Great Britain, first under grant no. NER/A/S/2000/01055 and subsequently under grant no. NE/B505738/1 (to MAC).

References

- Arzel L, Hehlen B, Dénoyer F, Currat R, Liss K-D and Courtens E 2003 *Europhys. Lett.* **61** 653–9
- Arzel L, Hehlen B, Tagantsev A K, Dénoyer F, Liss K D, Currat R and Courtens E 2002 *Ferroelectrics* **267** 317–22
- Basyuk T, Vasylechko L, Fadeev S, Syvorotka I I, Trots D and Niewa A 2009 *Radiat. Phys. Chem.* **78** S97–100
- Bednorz J G and Müller K A 1984 *Phys. Rev. Lett.* **52** 2289–92
- Birgeneau R J, Kjems J K, Shirane G and Van Uitert L G 1974 *Phys. Rev. B* **10** 2512–34
- Born M and Huang K 1954 *Dynamical Theory of Crystal Lattices* (Oxford: Clarendon)
- Carpenter M A 2007 *Am. Mineral.* **92** 309–27
- Carpenter M A, Buckley A, Taylor P A and Darling T W 2010a *J. Phys.: Condens. Matter* **22** 035405
- Carpenter M A, Howard C J, Kennedy B J and Knight K S 2005 *Phys. Rev. B* **72** 024118
- Carpenter M A, McKnight R E A, Howard C J, Zhou Q and Kennedy B J 2009 *Phys. Rev. B* submitted
- Carpenter M A and Salje E K H 1998 *Eur. J. Miner.* **10** 693–812
- Carpenter M A, Sinogeikin S V and Bass J D 2010b *J. Phys.: Condens. Matter* **22** 035404
- Carpenter M A, Sinogeikin S V, Bass J D, Lakshtanov D L and Jacobsen S D 2010c *J. Phys.: Condens. Matter* **22** 035403
- Cowley R A 1976 *Phys. Rev. B* **13** 4877–85
- Glynn T J, Harley R T, Hayes W, Rushworth A J and Smith S H 1975 *J. Phys. C: Solid State Phys.* **8** L126–8
- Grupp D E and Goldman A M 1997 *Science* **276** 392–4
- Guzhva M E, Lemanov V V and Markovin P A 2001 *Phys. Solid State* **43** 2146–53
- Guzhva M E, Lemanov V V, Markovin P A and Shuplygina T A 1998 *Ferroelectrics* **218** 93–101

- Hayward S A, Morrison F D, Redfern S A T, Salje E K H, Scott J F, Knight K S, Tarantino S, Glazer A M, Shuvaeva V, Daniel P, Zhang M and Carpenter M A 2005 *Phys. Rev. B* **72** 054110
- Hayward S A, Redfern S A T and Salje E K H 2002 *J. Phys.: Condens. Matter* **14** 10131–44
- Hayward S A and Salje E K H 1999 *Phase Transit.* **68** 501–22
- Hehlen B, Kallassy Z and Courtens E 1996 *Ferroelectrics* **183** 265–72
- Howard C J, Kennedy B J and Chakoumakos B C 2000 *J. Phys.: Condens. Matter* **12** 349–65
- Huijben M, Brinkman A, Koster G, Rijnders G, Hilgenkamp H and Blank D H A 2009 *Adv. Mater.* **21** 1665–77
- Itoh M and Wang R 2000 *Appl. Phys. Lett.* **76** 221–3
- Itoh M and Wang R 2003 *J. Phys. Soc. Japan* **72** 1310–1
- Itoh M, Wang R, Inaguma Y, Yamaguchi T, Shan Y-J and Nakamura T 1999 *Phys. Rev. Lett.* **82** 3540–3
- Itoh M, Yagi T, Uesu Y, Kleemann W and Blinc R 2004 *Sci. Tech. Adv. Mater.* **5** 417–23
- Leisure R G, Foster K, Hightower J E and Agosta D S 2004 *Mater. Sci. Eng. A* **370** 34–40
- Lemanov V V, Smirnova E P, Syrnikov P P and Tarakanov E A 1996 *Phys. Rev. B* **54** 3151–7
- Luo X and Wang B 2008 *J. Appl. Phys.* **104** 073518
- McKnight R E A, Carpenter M A, Darling T W, Buckley A and Taylor P A 2007 *Am. Miner.* **92** 1665–72
- McN Alford N, Breeze J, Wang X, Penn S J, Dalla S, Webb S J, Ljepojevic N and Aupi X 2001 *J. Eur. Ceram. Soc.* **21** 2605–11
- Ménoret C, Kiat J M, Dkhil B, Dunlop M, Dammak H and Hernandez O 2002 *Phys. Rev. B* **65** 224104
- Migliori A and Sarrao J L 1997 *Resonant Ultrasound Spectroscopy: Applications to Physics, Materials Measurements and Nondestructive Evaluation* (New York: Wiley)
- Migliori A, Sarrao J L, Visscher W M, Bell T M, Lei M, Fisk Z and Leisure R G 1993 *Physica B* **183** 1–24
- Moussa S M, Kennedy B J, Hunter B A, Howard C J and Vogt T 2001 *J. Phys.: Condens. Matter* **13** L203–9
- Müller K A, Berlinger W and Slonczewski J C 1970 *Phys. Rev. Lett.* **25** 734–7
- Müller K A, Berlinger W and Tosatti E 1991 *Z. Phys. B* **84** 277–83
- Noheda B 2002 *Curr. Opin. Solid State Mater. Sci.* **6** 27–34
- Sathe V G and Dubey A 2007 *J. Phys.: Condens. Matter* **19** 382201
- Schnelle W, Fischer R and Gmelin E 2001 *J. Phys. D: Appl. Phys.* **34** 846–51
- Schreuer J and Thybaut C 2005 *Proc. IEEE Ultrason. Symp.* **2005** 695–8
- Schreuer J, Thybaut C, Prestat M, Stade J and Haussühl S 2003 *Proc. IEEE Ultrason. Symp.* **2003** 196
- Schwingschlögl U and Schuster C 2009 *Chem. Phys. Lett.* **467** 354–7
- Scott J F and Ledbetter H 1997 *Z. Phys. B* **104** 635–9
- Terhune R W, Kushida T and Ford G W 1985 *Phys. Rev. B* **32** 8416–9
- Yagi T, Kasahara M, Tsujimi Y, Yamaguchi M, Hasebe H, Wang R and Itoh M 2002 *Physica B* **316/317** 596–9
- Yamaguchi M, Yagi T, Wang R and Itoh M 2001 *Phys. Rev. B* **63** 172102
- Zuccaro C, Winter M, Klein N and Urban K 1997 *J. Appl. Phys.* **82** 5695–704